Multi-process integration of nanoscale polymer and metal 3D printing for multi-material micro-optics

Jungho Choi,[a] Nikolas T. Roeske,[b] Mohanalingam Kathaperumal,[c,d] Sourabh K. Saha,[a*]

[a]Scalable Technologies for Advanced Manufacturing Lab, George W. Woodruff School of Mechanical Engineering, Georgia Institute of Technology, 801 Ferst Dr, Atlanta, GA 30332, USA

[b]Institute for Matter and Systems, Georgia Institute of Technology, Atlanta, GA 30332, USA

[c]3D Systems Packaging Research Center, Georgia Institute of Technology, Atlanta, GA 30332, USA

[d]School of Electrical and Computer Engineering, Georgia Institute of Technology, Atlanta, GA 30332, USA

[*]Corresponding author email: ssaha8@gatech.edu

Published on engrXiv: July 2026

Abstract

The ability to integrate different materials on the same substrate can significantly expand the functionality of printed optical microsystems. However, integration is challenging due to the apparent incompatibility between polymer and metal nanoscale 3D printing techniques. Here, we demonstrate the printing of polymer and metal micro-optics on a copper-coated silicon wafer using two different nanoscale 3D printers based on photopolymerization and electrochemical deposition. We identify the challenges in integrating these techniques and present an optimized fabrication scheme that enables cross-platform hybrid printing. Our work establishes a practical way for hybrid polymer-metal additive manufacturing using commercially available high-resolution nanoscale 3D printers.

Keywords: Additive manufacturing, Direct laser writing, Two-photon lithography, Electrochemical metal deposition, Nanolithography.

1. Introduction

Optics-based microsystems are emerging as the next generation microsystems for data-heavy, resource-efficient, and quantum-enabled applications, such as data center computers, quantum computers, and quantum sensors [1]. A key bottleneck for adoption of these microsystems at scale is the lack of packaging techniques that can route light to, from, and within these devices [2]. Printed microscale optical elements, such as metallic micro-mirrors and polymeric micro-lenses, can provide the capability for co-packaging and advanced packaging of microsystems. However, multi-material microscale 3D printers that have >10 μm resolution are generally incapable of producing the high-quality smooth surfaces that are required for optics. This challenge can be overcome with nanoscale 3D printers that can print polymeric or metallic 3D structures with smooth surfaces [3-5]. Despite the commercial availability of such printers, it is still challenging to produce hybrid metal-polymer 3D structures for micro-optics. This is primarily due to the apparent incompatibility of the underlying processing mechanisms of nanoscale 3D printers. Here, we overcome this challenge by investigating the sources of incompatibility and optimizing the processing conditions to enable the printing of hybrid metal-polymer 3D micro-optics.

Specifically, we have investigated the incompatibility of nanoscale polymer 3D printing via the two-photon polymerization (2PP) technique and nanoscale metal 3D printing via a tip-based electrochemical deposition (ECD) technique. The 2PP process has emerged as a popular technique for producing 3D polymer micro-structures by assembling nanoscale volumetric pixels (i.e., voxels). It relies on nonlinear absorption of light to produce voxels as small as 200 nm wide through localized curing of photoresists [6]. The 3D printing process involves scanning a beam of focused femtosecond laser within the photoresist to sequentially cure each voxel point-by-point. 2PP has been widely applied to produce micro-scale optical elements such as diffractive elements, zone plates, and curved lenses [7]. Similarly, tip-based ECD is a promising technique for producing metallic 3D structures with sub-micron voxels [8, 9]. In this process, voxels are produced through localized electrochemical reactions that convert solvated metal ions into metal atoms. The reactions are localized by using a microfluidic tip to deliver the metal ion solution at the printing zone. The 3D printing process involves scanning the tip within an electrolyte solution to sequentially deposit each voxel point-by-point. It has been used to produce microscale metallic 3D structures for electrical interconnects and sensors [5, 10].

In principle, multi-material 3D structures can be produced by integrating multiple 3D printing techniques through multi-step sequential printing on the same substrate [11, 12]. However, such an integration of 2PP and tip-based electrodeposition is challenging because 2PP requires an optically compatible substrate whereas ECD requires an electrically conductive metallic substrate. A metallic substrate can disrupt the polymerization behavior in 2PP by causing undesired interactions with the laser [13]. Here, we have used a Nanoscribe printer (for 2PP) and an Exaddon printer (for ECD) to enable integrated metal-polymer printing on the same copper-coated silicon wafer substrate. We have achieved this integration by characterizing the effect of the substrate on the fidelity of printing. Our optimized process enables hybrid metal-polymer nanoscale 3D printing through sequential printing of metal and polymer structures on the same substrate. Therefore, it can be widely applied to fabricate multi-material structures for packaging of optical microsystems.

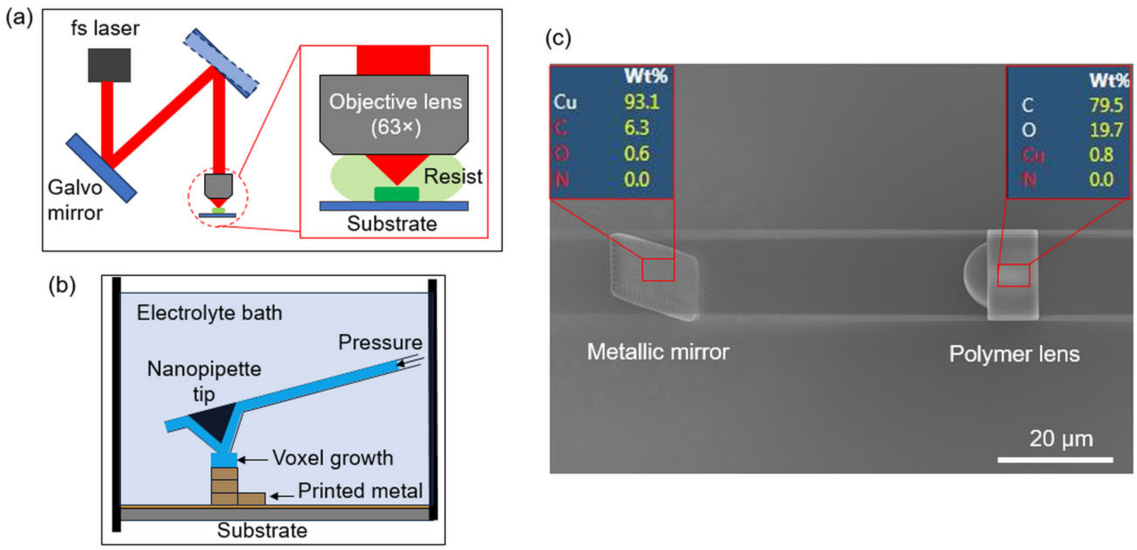

Figure 1: (a) Schematic of 2PP-based polymer printing with the Nanoscribe printer. (b) Schematic of electrochemical metal deposition with the Exaddon printer. (c) SEM image of the hybrid metal-polymer structures fabricated on a Cu-coated Si wafer through sequential printing with Exaddon and Nanoscribe.

2. Materials and methods

We printed benchmark polymer 3D micro-lenses using the commercially available Nanoscribe Photonic Professional GT2 system (Nanoscribe GmbH, Germany). This printer implements the scanning-based 2PP technique in which a near-IR femtosecond laser is rapidly scanned in the X-Y plane using a pair of galvanometric mirrors. Printing was performed with the IP-DIP resist available from Nanoscribe and with an oil immersion objective lens that had a magnification of 63× and a numerical aperture of 1.4. A schematic of the technique is shown in Fig. 1(a). Printing was performed in the dip-in mode wherein the objective lens is immersed in the resist. The laser power and the scanning speed were varied to characterize the effect of the substrate on the fidelity of printing. After exposure, the substrate was dipped into a bath of SU-8 developer solution for 15 minutes and then dipped into a bath of isopropyl alcohol for 10 minutes to remove the uncured resist. The substrate was then allowed to dry in ambient air before imaging. The geometry of the printed structures was characterized using a Hitachi SU8230 Scanning Electron Microscope (SEM). This SEM is also equipped with an Energy Dispersive X-ray (EDX) detector, which was used to characterize the elemental composition of the printed structures.

We printed micro-mirrors using the commercially available Exaddon CERES printer (Exaddon AG, Switzerland), which implements tip-based electrochemical metal deposition. A schematic of the technique is shown in Fig. 1(b). This printer enables scanning a fluidic probe that is immersed within an electrolyte bath. A mixture of sulfuric acid, hydrochloric acid, and deionized distilled water was used as the electrolyte. The probe (named Iontip from Exaddon) resembles the cantilever tip of an atomic force microscope (AFM), and it contains a hollow microfluidic channel. A $CuSO_4$ electrolyte solution is pumped through this channel and ejected out from the tip under pressure. The tip was scanned at a speed of 2 µm/s and the tip voltage for the electrochemical cell was -0.54 V. The localized metal ion delivery enables localized electrochemical reduction of copper (II) ions into metallic copper nanoparticles near the probe tip. By maintaining an initial probe–substrate separation of several hundred nanometers, the electrodeposited metal can grow in the vertical direction, forming a voxel and thereby enabling 3D printing. After printing, the substrate was dipped into a bath of deionized distilled water and then subsequently taken out and dried with a stream of nitrogen gas. The printed metallic structures were characterized using the SEM and the surface roughness was measured using a laser confocal microscope (Olympus LEXT).

3. Results and discussion

As illustrated in Fig. 1(c), we successfully printed the hybrid metal-polymer 3D structure on a copper-coated silicon wafer through sequential printing with two different printers. The metallic micro-mirror was fabricated with electrochemical metal deposition and the polymer micro-lens was printed with two-photon polymerization. The mirror was printed at a tilt angle of 45° with respect to the substrate and it was aligned to overlap the optical axis of the lens. Such a hybrid structure may be applied to route light between the on-chip direction (i.e., along substrate surface) and the vertical direction. With optimized printing parameters, we demonstrated that structures with accurate geometry can be printed on a single substrate through sequential printing first with the Exaddon and then with the Nanoscribe. The EDX analysis confirmed the successful fabrication of metallic copper micro-mirror and polymer lens within the hybrid structure. Specifically, the EDX data showed a significant proportion of copper (93% by weight) and carbon (79% by weight) in the printed regions for metal and polymer structures, respectively.

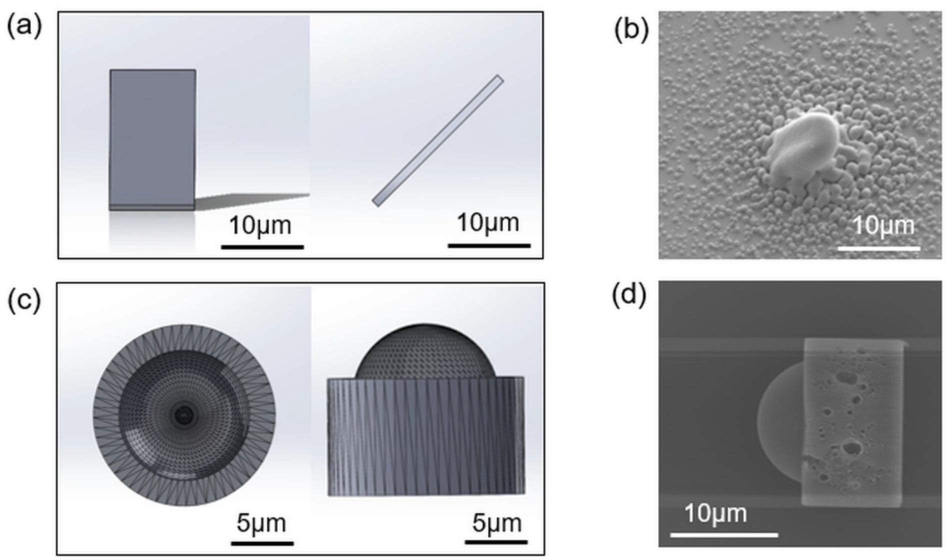

Figure 2: Defects arising from 2PP and ECD integration. (a) Model of the designed micro-mirror. (b) SEM image of a metallic micro-mirror printed with ECD on ITO-coated glass substrate depicting poor geometric fidelity. (c) Model of the designed micro-lens. (d) Top-down SEM image of a polymer micro-lens printed with 2PP on a Cu-coated Si wafer depicting bubbling defects on the top surface.

Our first step in developing an optimal sequential printing scheme was to identify the optimal ordering of the two processes, i.e., to identify which printer must be used first. On the Nanoscribe printer, dip-in 2PP is commonly performed on optically clear glass substrates that are coated with a thin film of indium tin oxide (ITO) [14]. This coating generates a partially reflective interface that aids in locating the focal plane of the laser. Incidentally, ITO is also electrically conductive, and it is reasonable to expect that it would be a compatible substrate for ECD. However, our tests demonstrated that ITO-coated glass substrates performed poorly during ECD. The designed size of the micro-mirror was 20 μm tall, 10 μm wide and 1 μm thick. As illustrated in Figs. 2(a) and (b), ECD on the ITO-coated surface produced a poorly defined structure with uncontrolled excessive copper deposition around it. It is noteworthy that past studies with the Exaddon printer have predominantly used highly conductive metallic films on the substrates, such as copper and gold films [8, 9]. When 2PP was performed on a copper-coated silicon wafer that was processed on the Exaddon, near-optimal printing was observed with some defects. Based on these tests, we determined that printing first with the Exaddon and then with the Nanoscribe on the same copper-coated silicon wafer was a promising approach for sequential printing.

Additional 2PP process optimization was necessary to achieve accurate geometries through sequential printing. The designed geometry of the polymer lens is shown in Fig. 2(c). The lens comprises a cylindrical base of diameter 15 μm and a hemispherical top with a diameter of 11 μm. To identify optimal processing conditions for printing on top of Cu-coated Si wafer, we varied the laser power and the Z-layer spacing (i.e., spacing along the vertical axis) and measured the diameter of the cylinder from top-down views. As shown in Figs. 3(a) and 3(b), power levels below 50% produced structures that were smaller than the designed geometry, whereas 50% power level led to accurate printing. The 100% power level represents an optical beam power of 53 mW. Further fine tuning of the geometry was achieved by varying the Z-layer spacing; 100 and 200 nm spacings produced the most accurate structures. Although these optimal parameters produced accurate structures with stand-alone 2PP, defective prints were produced when 2PP was performed sequentially after electrochemical deposition with the Exaddon printer. Specifically, we observed that bubbles were formed in the resist due to localized boiling, as is evident from the SEM image shown in Fig. 2(d). We hypothesized that the surface of the copper-coated substrate is altered upon exposure to the electrolyte bath in the Exaddon, thereby requiring further optimization of the 2PP process parameters.

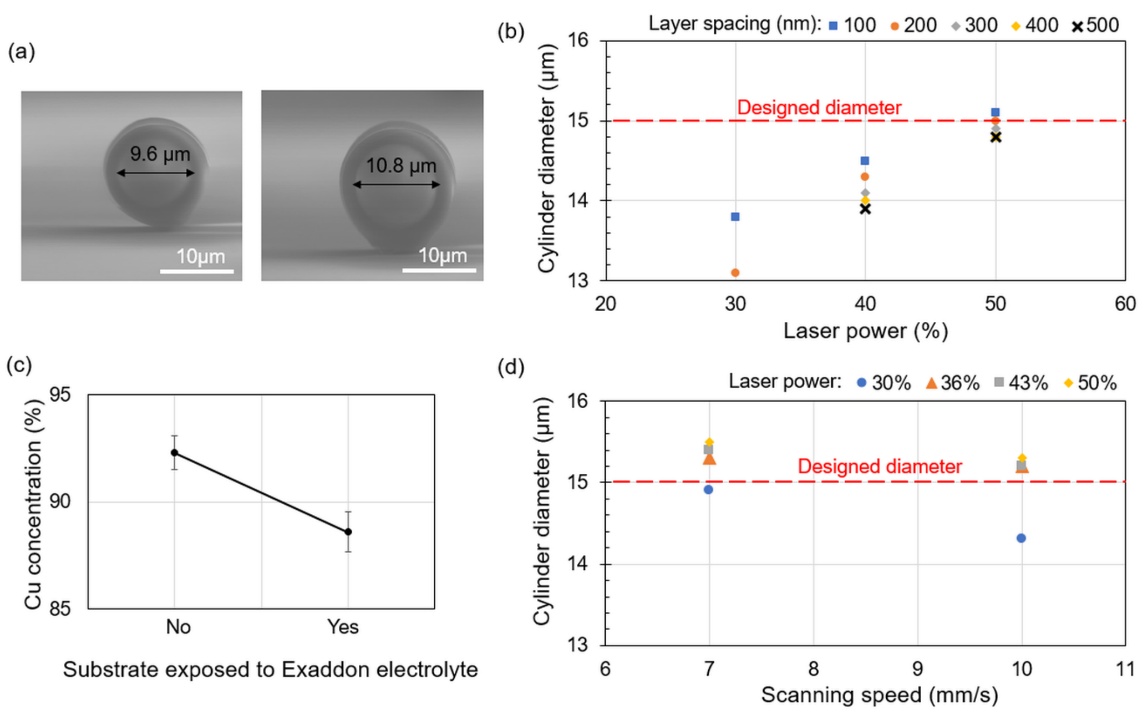

Figure 3: Optimization of 2PP performed with the Nanoscribe. (a) SEM images depicting front-view of micro-lenses printed with 30% (left) versus 50% (right) power, 100 nm layer spacing, and 10 mm/s scanning speed. (b) Diameter of cylindrical base of micro-lenses versus laser power at scanning speed of 10 mm/s and varying layer spacings during printing on Cu-coated Si wafer unexposed to Exaddon electrolyte. (c) Energy-Dispersive X-ray (EDX) analysis of Cu-coated Si wafer before and after exposure to the electrolyte bath in the Exaddon. (d) Cylinder diameter versus laser scanning speed at varying laser powers and with 100 nm layer spacing during printing on Cu-coated Si wafer that was exposed to the Exaddon electrolyte.

We have verified our hypothesis by measuring the concentration of copper on the substrate before and after exposure of the substrate to the electrolyte of the Exaddon printer. The EDX data, summarized in Fig. 3(c), confirmed that exposure to the electrolyte bath reduces the amount (i.e., thickness) of copper on the substrate. We suspect that the boiling-based bubbles form in the resist because the heat dissipation through the substrate slows down on a thinner copper film due to its lower in-plane thermal conductance. Boiling-based bubble defects are commonly observed during 2PP when printing is performed at high exposure dosages [15, 16]. To prevent bubble formation, we performed printing with lower laser power and lower beam scanning speeds. It is expected that such a combination of parameters would lower the amount of heat absorbed and would also allow the heat to dissipate over a longer duration. As expected, printing with 30% power (instead of 50%) and at 7 mm/s scanning speed (instead of 10 mm/s) produced accurate structures with no bubbles (Fig. 3(d)). This optimized set of parameters enables sequential printing of polymer structures via 2PP on the same substrate that has been previously processed through the Exaddon printer.

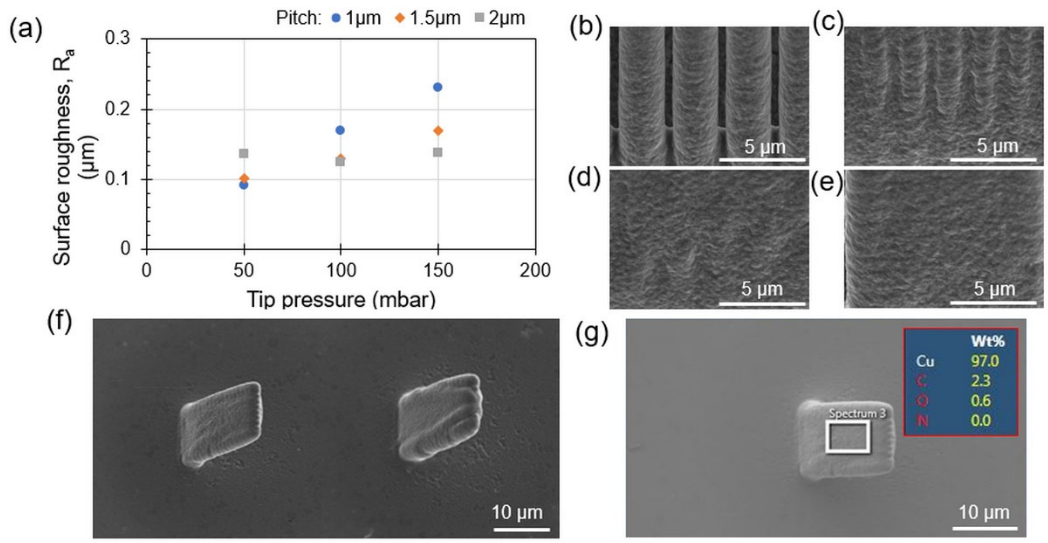

Figure 4: Optimization of electrochemical metal deposition performed with the Exaddon printer. (a) Surface roughness of micro-mirrors versus tip pressure at various pitches. (b-e) SEM images of the micro-mirrors printed with decreasing pitch (3, 2, 1.5, and 1 μm) and 50 mbar pressure. (f) SEM images of micro-mirrors printed with 1 μm pitch and 50 mbar tip pressure (left) versus 100 mbar pressure (right). (g) EDX analysis of micro-mirror printed with 1 μm pitch and 50 mbar pressure.

We have further optimized the ECD process to produce smooth surfaces on the metal micro-mirrors. To minimize surface roughness while maintaining geometric fidelity, we systematically varied the fluidic pressure through the tip and the voxel pitch. As shown in Fig. 4(a), the smoothest surface was achieved at a tip pressure of 50 mbar and a pitch of 1 μm. Figures 4(b)–(e) show the evolution of the surface profile as the pitch decreases from 2.5 μm to 1.0 μm at a pressure of 50 mbar. As the pitch decreases, voxel overlap increases and the surface becomes progressively smoother. However, even at 1 μm pitch, the tip pressure strongly affects the voxel size. Increasing the tip pressure enlarges the deposited voxel, which leads to excessive overlap and surface degradation. This trend is evident in Fig. 4(f), where the mirror printed at 100 mbar (right) exhibits higher surface roughness than the mirror printed at 50 mbar (left). This observation is consistent with the expectation that larger voxels are produced at higher tip pressure. Finally, EDX analysis confirmed that the printed mirror was a copper-rich metallic structure (Fig. 4g).

4. Conclusions

In this work, we have demonstrated a practical strategy for fabricating hybrid polymer–metal microstructures by enabling cross-platform compatibility between two nanoscale 3D printing techniques. By systematically optimizing the process parameters for both two-photon polymerization and localized electrochemical metal deposition, we successfully fabricated polymer micro-lenses and metallic copper micro-mirrors on the same copper-coated silicon wafer substrate. We demonstrated that the substrate incompatibility between polymer and metal printing can be mitigated by performing electrochemical deposition before two-photon polymerization and through targeted printing parameter optimization to account for substrate modifications after electrochemical deposition. Our study provides a scalable pathway for fabricating multifunctional optical microsystems that combine structural polymers and metals.

Acknowledgements

This work was funded by the 3D Systems Packaging Research Center at the Georgia Institute of Technology and the authors would like to acknowledge the support of the consortium members of the center. Imaging and printing were performed at the Georgia Tech Institute for Matter and Systems, a member of the National Nanotechnology Coordinated Infrastructure (NNCI), which is supported by the National Science Foundation (ECCS-2025462).

References

[1] Ning S, Zhu H, Feng C, Gu J, Jiang Z, Ying Z, et al. Photonic-electronic integrated circuits for high-performance computing and ai accelerators. Journal of Lightwave Technology. 2024.

[2] Baek K, Kim M, Kim HS, Ahn J, So H. Advanced Optical Integration Processes for Photonic-Integrated Circuit Packaging. Advanced Materials Technologies. 2025:e01848.

[3] Wang H, Zhang W, Ladika D, Yu H, Gailevičius D, Wang H, et al. Two-Photon Polymerization Lithography for Optics and Photonics: Fundamentals, Materials, Technologies, and Applications. Advanced Functional Materials. 2023:2214211.

[4] Yu S, Du Q, Mendonca CR, Ranno L, Gu T, Hu J. Two-photon lithography for integrated photonic packaging. Light: Advanced Manufacturing. 2024;4:486-502.

[5] Lodhi I, Brown DK, Gajula D, Haile BD, Myers DR, Lam WA, et al. Integrating 3D-Printed Metal and Polymer Geometries with CMOS Microdevices toward MEMS High-Resolution Lateral Force Sensing. Additive Manufacturing. 2026:105085.

[6] Baldacchini T. Three-dimensional microfabrication using two-photon polymerization: fundamentals, technology, and applications: William Andrew, 2015.

[7] Gonzalez-Hernandez D, Varapnickas S, Bertoncini A, Liberale C, Malinauskas M. Micro-Optics 3D Printed via Multi-Photon Laser Lithography. Advanced Optical Materials. 2023;11:2201701.

[8] Ercolano G, van Nisselroy C, Merle T, Vörös J, Momotenko D, Koelmans WW, et al. Additive manufacturing of sub-micron to sub-mm metal structures with hollow AFM cantilevers. Micromachines. 2020;11:6.

[9] Schürch P, Osenberg D, Testa P, Bürki G, Schwiedrzik J, Michler J, et al. Direct 3D microprinting of highly conductive gold structures via localized electrodeposition. Materials & Design. 2023;227:111780.

[10] Soto-Valle G, Joshi M, Mensah Y, Roeske N, Lynch CA, Cressler JD, et al. Novel Low-Loss Shielded Interconnects for D-Band/Sub-THz Applications Using Microscale Metal Printing Technologies. IEEE Microwave and Wireless Technology Letters. 2025.

[11] Saha SK, Uphaus TM, Cuadra JA, Divin C, Ladner IS, Enstrom KG, et al. Kinematic fixtures to enable multi-material printing and rapid non-destructive inspection during two-photon lithography. Precision Engineering. 2018;54:131-7.

[12] MacDonald E, Wicker R. Multiprocess 3D printing for increasing component functionality. Science. 2016;353:aaf2093.

[13] Rekštytė S, Žukauskas A, Purlys V, Gordienko Y, Malinauskas M. Direct laser writing of 3D polymer micro/nanostructures on metallic surfaces. Applied Surface Science. 2013;270:382-7.

[14] Bunea A-I, del Castillo Iniesta N, Droumpali A, Wetzel AE, Engay E, Taboryski R. Micro 3D printing by two-photon polymerization: configurations and parameters for the nanoscribe system. 2 ed: MDPI. p. 164-80.

[15] Mueller JB, Fischer J, Mange YJ, Nann T, Wegener M. In-situ local temperature measurement during three-dimensional direct laser writing. Applied Physics Letters. 2013;103:123107.

[16] Saha SK, Divin C, Cuadra JA, Panas RM. Effect of proximity of features on the damage threshold during submicron additive manufacturing via two-photon polymerization. Journal of Micro and Nano-Manufacturing. 2017;5.